Experiments on a light duty SCR test exhaust system using ammonia gas to provide data for validation of a CFD model

Benjamin, S.F. , Gall, M. , Sturgess, M.P. and Roberts, C.A.

Original citation & hyperlink:
Benjamin, S.F. , Gall, M. , Sturgess, M.P. and Roberts, C.A. (2011) 'Experiments on a light duty SCR test exhaust system using ammonia gas to provide data for validation of a CFD model' in Internal Combustion Engines: Improving Performance, Fuel Economy and Emissions (pp. 219-234). Cambridge: Woodhead Publishing.
http://dx.doi.org/10.1533/9780857095060.6.217

ISBN: 9780857095060/ 9780857092052

Additional information: This research was funded by EPRSC.
Grant number: EP/F036175/1.
Project title: Modelling NOx Reduction by Selective Catalytic Reduction (SCR) appropriate for Light-Duty Vehicles under Steady State and Transient Conditions.

Experiments on a light duty SCR test exhaust system using ammonia gas to provide data for validation of a CFD model

S.F. Benjamin, M. Gall, M. P. Sturgess & C. A. Roberts

Automotive Engineering Applied research Group, Faculty of Engineering and Computing, Coventry University, UK

ABSTRACT

Modelling of reactions in SCR catalysts is a challenging process, but kinetic schemes are available in the literature derived from reactor tests with specific catalysts. This paper reports experiments on a light duty common rail diesel engine and test exhaust fitted with copper zeolite SCR. The experiments aimed to provide data for CFD model validation. Four different lengths of SCR catalyst brick were investigated: 30, 45, 75 and 91 mm. The tests were undertaken for NO_2:NOx ratios of 0.05, 0.46, 0.62 and 0.82 approximately. Three ammonia dosing levels were investigated. These were deficient ammonia, i.e. NH_3:NOx ratio about 0.5, stoichiometric, where the ratio was near 1.0 and excess ammonia, ratio greater than 1.0. A 1D steady state CFD model using the porous medium approach was developed based on available kinetics. Most of the experiments were at low exhaust temperature around 220 °C but a case near 300 °C was also investigated. Comparison of CFD predictions with measurements showed that the kinetic scheme gave moderate predictions with a stoichiometric ammonia supply to the exhaust and an NO_2:NOx ratio near 50 % but that the model was inadequate for other conditions. There was notably more NOx consumption than predicted for short bricks and for deficient ammonia levels. The data were obtained in a real engine exhaust at much higher space velocities than those used to derive the kinetics; this study is therefore a strong test of the kinetic model. Attempts to modify the CFD model to provide closer agreement with experimental observations are ongoing.

NOTATION

A_i	Stoichiometric coefficient for species i
A_V	Reactor surface area per unit volume (m^2/m^3)
$C_{i\ Gas}$	Concentration of species i in the gas phase (mass fraction)
$C_{i\ Sol}$	Concentration of species i in the pore phase (mass fraction)
$K_{i\ m}$	Mass transfer coefficient of species i (m/s)
L	Channel length (m)
M	Molecular mass (kg/mol) for species i
P	Pressure (N/m^2)
R_i	Reaction rate for species i (mol/mol-site/s)

$R_{i\ Tot}$	Total reaction rate from multiple reactions for each species
t	Time (s)
T	Temperature (K)
U_S	Superficial velocity, i.e. [channel velocity/ε] (m/s)
V_W	Pore volume per unit reactor volume (m^3/m^3)
α	Resistance coefficient
β	Resistance coefficient
ε	Porosity of the substrate
ρ	Density of air (kg/m^3)
θ	Fraction of catalytically active sites occupied by ammonia
Ω	Number of reaction sites (mol-sites/m^3)

1 INTRODUCTION

Recent years have seen a large increase in the number of light duty diesel vehicles. The engines run lean, are economical on fuel and low on regulated emissions. Ever more stringent emissions regulations, however, have led to the need for advanced NOx control measures for such engines. The preferred technology is the use of selective catalytic reduction (SCR) of NOx with ammonia. The ammonia is usually supplied into the exhaust stream by a spray of aqueous urea. At sufficiently high temperature, the urea droplets evaporate and the urea breaks down into ammonia and also HCNO, which in turn is hydrolysed to ammonia. The chemical reactions that take place within the SCR catalyst brick are complex. The NOx, a mixture of NO and NO_2, reacts with the ammonia in a reaction scheme that consists of multiple reactions. The main SCR reactions are commonly referred to as the standard, slow and fast reactions. There is a fourth reaction that leads to the formation of N_2O and there are numerous side reactions associated with the main scheme that can lead to the formation of ammonium nitrite and nitrate. Additionally, the ammonia itself can oxidise on the catalyst in the lean exhaust stream and NO can be oxidized to NO_2 with the latter reaction being reversible. The balance between the reactions is dependent upon the temperature and on the NO_2:NOx ratio in the exhaust as well as on the amount of ammonia supplied. The ammonia available for the reactions is dependent upon the rate of adsorption and desorption of ammonia at the catalyst surface. Reactions with NO_X can only take place on active catalyst sites occupied by ammonia. Some authors propose the existence of more than one type of site, for example Schwidder et al. (1) and Kamasamudram et al. (2), but Olsson et al. (3) have provided a comprehensive scheme based on only one type of site and that is advantageous in terms of modelling simplicity and computational efficiency.

The models are developed for specific types of catalyst, vanadium originally, for example (4), and (5) where vanadium and zeolite are compared, but now usually for either copper zeolite (3) or iron zeolites (6). They are developed in reactor tube tests, often under low space velocity conditions, for example 18,400 h^{-1} in the case of Olsson et al. (3). A CFD model can be set up using one of these kinetic schemes. The porous medium approach (7) is appropriate and computationally efficient for catalyst modelling as it is unnecessary to model individual substrate channels. Data from conditions nearer to those in real automotive exhausts are needed to validate such models based on reactor kinetics. Of particular interest are the reactions occurring inside the catalyst brick and this can be investigated by measuring at the exit from short catalyst bricks. Luo et al (8) have investigated the spatial resolution of the SCR reactions but over an iron zeolite catalyst. Watling et al. (9) have tested a model for copper zeolite, but the emphasis was on transient studies over engine test cycles.

Experiments have been carried out here on a test exhaust fitted to an engine on a test bed. The exhaust was fitted with copper zeolite SCRs. Preliminary results were reported in (10). Four different lengths of SCR catalyst brick have now been

investigated and the tests have been undertaken for NO_2:NOx ratios of 0.05, 0.46, 0.62 and 0.82 approximately. Three ammonia dosing levels were investigated: deficient ammonia, stoichiometric ammonia and excess ammonia. Ammonia gas was used to make the dosing controllable and to simplify the CFD validation as no urea droplet or hydrolysis models were required. The exhaust temperature was low near 220 °C, which is typical of an automotive Diesel exhaust, but higher temperatures would be experienced under high load so a set of additional tests was carried out near 300 °C.

The experiments are described in this paper and the data obtained are presented. The experiments were carried out under real engine exhaust conditions at space velocities in excess of 100,000 h^{-1}. Details are given of the CFD model and the data are compared with predictions from the model. This is a critical test of kinetics obtained under very different space velocity conditions (3). The implications are discussed and modelling changes are proposed.

2 EXPERIMENTAL TEST RIG AND PROCEDURE

The experiments were carried out on the exhaust of an engine mounted on a 150 AC dynamometer. The engine was a 1998cc 4-cylinder light-duty diesel engine with a common rail fuel injection system, an intercooled turbocharger, and EGR. The latter was de-activated so that high levels of NOx were available from the engine for the purposes of the measurements. Downstream of the engine a DPF removed any soot and particulate matter. The NO_2:NOx ratio supplied to the SCR in the exhaust was controlled by the length of a DOC placed downstream of the DPF. The DPF was deliberately placed upstream of the DOC in the experimental test rig so that NO_2 produced in the DOC was not reduced by soot.

Fig. 1 shows a schematic diagram of the test rig. Ammonia gas was supplied as 5% NH_3 gas in nitrogen and was injected into the exhaust downstream of the DOC. The three different NH_3: NOx injection ratios were: 0.5, deficient ammonia; 1.0, stoichiometric ammonia; > 1.0, excess ammonia.

Downstream of the DOC the exhaust passes through an expansion box and converging nozzle. This promotes the mixing of the injected ammonia gas with the exhaust and provides a uniform velocity profile at the inlet to a long diffuser with a ten degree angle. The latter assists the flow in remaining attached within the diffuser and hence a uniform velocity profile is supplied at the inlet to the SCR catalyst brick. In this way it is possible to regard the data as being generated in a 1D system and to model the data with a 1D-CFD model. A 1D-CFD model once developed can be readily applied to any 3D case using the porous medium approach.

The system was lagged so that the temperature of the exhaust gas supplied to the SCR was above 200 °C. The SCR catalyst was a form of copper zeolite, and had been conditioned for 24 hours in a hydrothermal oven at 650 °C. The washcoated ceramic catalyst bricks were 115 mm in diameter and the investigated lengths were 30, 45, 75 and 91 mm. The volume of the 91 mm brick was approximately 1 litre.

Emissions were measured using a Horiba EXSA 1500 gas analyser at the engine outlet; this monitored the total NOx emissions from the engine to ensure consistency of engine performance throughout the tests, which were of about three hours duration, including an engine warm up period. A Horiba MEXA 1170 NX gas analyser was used to measure NOx and NH_3 levels before and after the SCR brick. Previous work on NOx measurements in the presence of ammonia has shown that the measured NOx values can be erroneous because ammonia can react with NO_2 on the analyser's internal NOx converter catalyst (11). To avoid this, ammonia

scrubbers were fitted within the MEXA analyser. The scrubbers were designed to remove ammonia before the sample gas entered the NOx converter within the analyser. The scrubbers had an estimated lifetime of 50,000 ppm hours and were changed regularly during the experimental programme.

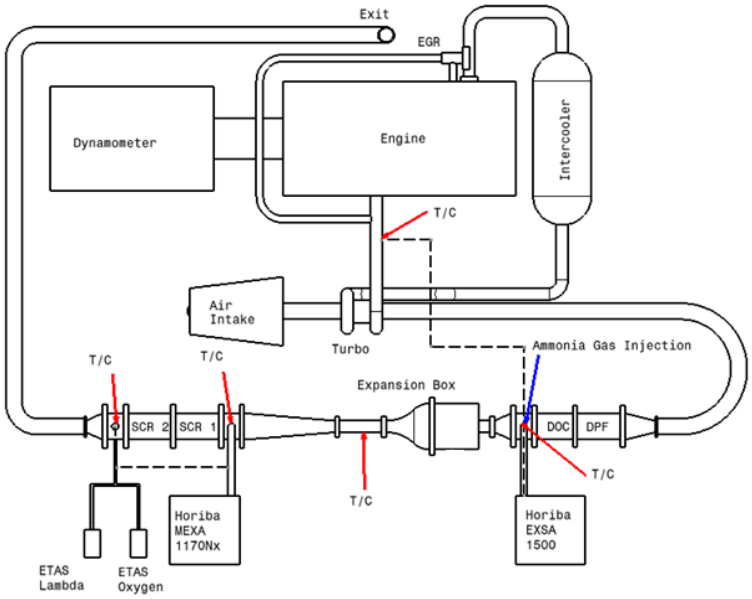

Figure 1: Exhaust test rig (10). T/C shows location of thermocouple.

An engine condition of 1500rpm with 6 bar brake mean effective pressure (BMEP) was the condition for the majority of the experiments and this provided an exhaust temperature near 220 °C at inlet to the SCR, which is typical of an automotive Diesel exhaust system. A second condition of 1500 rpm and 9 bar BMEP achieved a temperature of about 300 °C for one set of tests.

The test procedure to obtain steady state emissions values was similar to that described in a previous paper (10). The engine was warmed up for a period of about 40 minutes until the temperature was stable. The MEXA analyser was calibrated and was used to sample upstream of the SCR to establish the three ammonia input levels for the experiment corresponding to three selected flow meter settings. After that the ammonia was turned off, the system was allowed to purge and the NOx, NO and NO_2 input levels were checked upstream of the SCR in the absence of ammonia. The MEXA analyser was then moved to sample downstream of the SCR. The test procedure is illustrated by Figs. 2 (a) and (b). With the MEXA analyser in ammonia mode the levels of NOx and NH_3 were measured as they approached steady state for the three different ammonia input rates. The steady state values can be read from Fig. 2 (a) just after 7350s, 7700 s and 8100 s. After the ammonia was turned off at about 8200 s in Fig. 2 (a) the NOx level was monitored until it returned to the input level. This was assumed to indicate that the SCR was empty of stored ammonia. After a calibration check, the timed experiment was repeated with the MEXA in NO_2 mode. The logged trace is shown in Fig. 2 (b) for NOx, NO and NO_2. The levels are read just after 9750, 10100 and 10500 seconds. The ammonia injection was turned off after 10600 s and the NOx, NO and NO_2 levels were allowed to return to their input values, indicating

all accessible stored NH_3 had been utilized. The MEXA analyser was returned to its upstream sampling position and a final calibration and check on the ammonia input levels was made to complete the experiment.

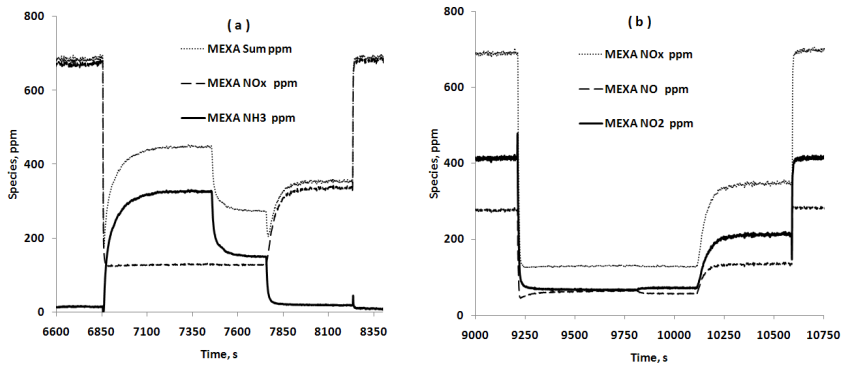

Figure 2: Illustration of logged traces obtained from test procedure: (a) Measurements with MEXA analyser of NOx and NH_3 levels downstream of SCR for 3 different NH_3 input levels (b) Measurements of NO and NO_2 levels downstream of SCR for 3 three different NH_3 input levels.

The total mass flow rate of exhaust, the % oxygen level in the exhaust and the temperature of the exhaust at inlet to the SCR were recorded as they were required as input information for a CFD simulation of the steady state tests. Temperature measurements were obtained from thermocouples located as indicated in Fig. 1.

3 CFD MODEL

The CFD package used was Star-CD Version 4.14 and the monolithic catalysts were modelled using the porous medium approach (7). The mesh used to represent the monolith was a simple rectangular block of 3 cells $\times$ 3 cells with 50 cells along the length of the 91 mm porous medium that represented the catalyst brick. Each of those cells was 1.82 mm in length. The SCR kinetics used for the CFD model can be found in full in the literature (3), where all the reaction rate constants are specified. The scheme contains rates for adsorption and desorption of ammonia and the following SCR reactions:

Standard SCR: $4NH_3 + 4NO + O_2 \rightarrow 4N_2 + 6H_2O$ [1]

Fast SCR: $2NH_3 + NO + NO_2 \rightarrow 2N_2 + 3H_2O$ [2]

Slow SCR: $4NH_3 + 3NO_2 \rightarrow 3.5N_2 + 6H_2O$ [3]

N_2O Formation: $2NH_3 + 2NO_2 \rightarrow N_2 + N_2O + 3H_2O$ [4]

Ammonia oxidation and reversible NO oxidation reactions are also included in the scheme, and are specified by reactions [5] and [6] respectively:

$$2NH_3 + 1.5O_2 \rightarrow N_2 + 3H_2O \quad [5]$$

$$NO + 0.5O_2 \leftrightarrow NO_2 \quad [6]$$

Additional side reactions such as nitrate formation are not included in the scheme, although these may occur at temperatures below 200 °C. For this reason the experiments were carried out near 220 °C.

In the CFD model heat sources due to the SCR reactions were neglected but heat transfer between the gas phase and the porous medium is managed within Star-CD by specification of the thermal conductance per unit volume. Allowance was made in the heat transfer coefficient value for higher Nusselt numbers downstream of the channel entrance (12). The energy equations are solved for the fluid and solid phases of the porous medium that represents the SCR monolith. The heat conduction within the solid phase of the monolith can be calculated within Star-CD; the density, thermal conductivity and specific heat of the washcoated substrate walls are specified to the code along with the substrate porosity.

By analogy with heat transfer, the mass transfer coefficients were corrected to allow for higher Sherwood numbers downstream of the channel entrance. A recent paper (13) has attempted to quantify the mass transfer effect. Mass transfer of species between gas and pore phases was modelled within the fluid phase of each computational cell and sources and sinks of species due to reactions were determined within the coding of the scalar source user subroutine. The species modelled were O_2, NO, NO_2, NH_3, N_2O for both gas and pore phases and θ, fraction of active sites occupied by NH_3.

Equations [7] and [8] are the transport equations for the scalar species that represent the reactants; the source terms are on the RHS of each equation. The gas phase concentrations are controlled by mass transfer in equation [7] but the pore phase concentrations are influenced both by mass transfer and reaction rates in equation [8]. Reaction rates R_i are calculated using the pore phase concentrations.

$$\varepsilon \frac{\partial}{\partial t}\left[\rho_{Air} C_{iGas}\right] + \frac{\partial}{\partial z}\left[\rho_{Air} U_S C_{i\,Gas}\right] = -K_{i\,m}\rho_{Air} A_V [C_{i\,Gas} - C_{i\,Sol}] \quad [7]$$

$$\varepsilon \frac{\partial}{\partial t}[\rho_{Air} C_{iSol}] = \{K_{i\,m}\rho_{Air} A_V [C_{i\,Gas} - C_{i\,Sol}] + MR_{i\,Tot}\}[\frac{\varepsilon}{V_w}] \quad [8]$$

The net total reaction rate in equation [8] is calculated by multiplying the reaction rate for each reaction in which the species participates by the appropriate stoichiometric coefficient, A_i. The surface coverage relationship for ammonia sites stated by Olsson et al. (3) is given by equation [9].

$$\frac{\partial \theta}{\partial t} = \sum[A_i R_i] \quad \text{mol/mol-site/s} \quad [9]$$

This is interpreted within the Star-CD CFD model by equation [10], where the net rate of storage of ammonia is then found from the balance between adsorption, desorption and consumption:

$$\varepsilon \rho_{Air} \frac{\partial \theta}{\partial t} = \frac{\varepsilon \rho_{Air}}{\Omega}[R_{ads} - R_{des} - R_{con}] \quad [10]$$

In equation [10] all rates are in mol/m^3 monolith/s and the ammonia capacity of the substrate has value Ω mol-sites/m^3 monolith. Olsson et al. (3) use a value of 200 mol-sites/m^3 substrate. A nominal value of 400 mol-sites/m^3 has been used here. In the CFD model, however, the number of available active sites is determined by the local temperature of the solid phase by application of the factor $(293/T)^2$. This gives an approximate working value of 140 mol-sites/m^3 at 220 °C and 105 mol-sites/m^3 at 300 °C. The multiplier of the ammonia desorption rate activation energy is (1 – 0.98θ), exactly as specified by Olsson et al. (3) even though this is different from the values (1–0.31θ) used by Chi et al. (4) and (1–0.545θ) used by Chatterjee et al. (5).

Pressure loss along the porous medium is calculated within Star-CD using equation [11] with appropriate resistance coefficients α and β.

$$\frac{\Delta P}{L} = -\alpha U_S^2 - \beta U_S \qquad [11]$$

The inlet conditions for the steady state CFD simulations are given in Table 1. These were obtained from the measurements at the entrance to the SCR on the engine test bed. The NO and NO_2 values are representative of the engine test bed experiments for the four different brick lengths. The output from the CFD simulation for the four SCR brick lengths investigated was obtained from a single run for each NH_3:NOx ratio investigated.

Table 1: Parameters for steady state CFD simulations at 220 and 300 °C.

Config.	Temp.	Mass flow rate g/s	O_2	NO	NO_2	NH_3	NH_3:NOx	NO_2:NOx
2 DOC	239.5	29.8	0.1286	100	454	287	0.52	0.82
						576	1.04	
						717	1.29	
1 DOC	233	29.8	0.1286	217	353	277	0.49	0.62
						561	0.98	
						764	1.34	
1 DOC	211	31.1	0.1348	323	275	294	0.49	0.46
						603	1.01	
						906	1.52	
0 DOC	227	29.8	0.1286	555	28	293	0.5	0.05
						580	0.99	
						721	1.24	
2 DOC	299	31.8	0.0944	245	485	353	0.48	0.66
						703	0.96	
						876	1.20	

4 MEASUREMENTS IN THE TEST EXHAUST

The steady state measurements obtained from the experiments at 220 °C are plotted in Fig. 3 as consumed ratios. The ratio of NO_2 consumed to NOx consumed and the ratio of NO consumed to NOx consumed are both plotted as a function of the NO_2:NOx ratio supplied to the SCR.

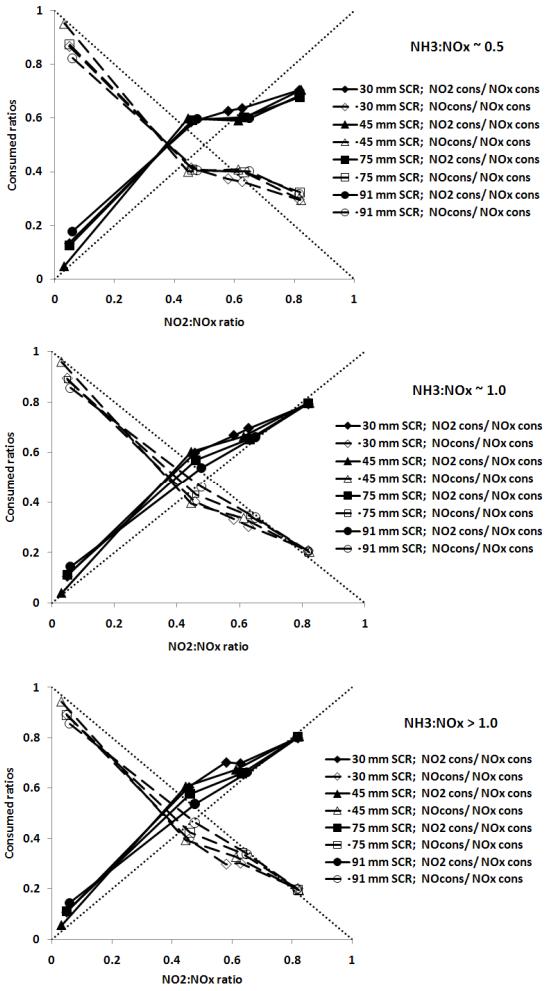

Figure 3: Ratio of NO_2 consumed to NOx consumed and of NO consumed to NOx consumed plotted as a function of inlet NO_2:NOx ratio for 220 °C tests.

The three graphs in Fig. 3 are for NH_3:NOx ratios near 0.5, 1.0, and > 1.0, i.e. for deficient, stoichiometric and excess ammonia. It can be seen that when the amount of ammonia supplied is deficient, and the NO_2:NOx ratio supplied is low, NO_2 is preferentially consumed but when the supplied ratio is near 0.62, the amount consumed is proportionate. When the supplied ratio is high, near 0.82, NO_2 consumption is restricted. In the lower two graphs of Fig. 3, when the supply of ammonia was adequate or in excess, the consumption of NO_2 is proportionate at 0.82, which was the highest NO_2:NOx ratio investigated. At lower NO_2:NOx ratios, there is preferential consumption of NO_2.

There is preferential NO consumption for NH_3:NOx near 0.5 when the NO_2:NOx ratio supplied is high, 0.82. Consumption of NO is proportionate for that ratio the when

ammonia supply is adequate or in excess. Under all other conditions NO consumption is restricted. These observations on the data in Fig. 3 are summarised in Table 2.

Table 2: Summary of combined effect of NO_2:NOx and NH_3:NOx ratios on the ratio of consumed NO_2 (ΔNO_2) to consumed NOx

	NO_2:NOx Low	**NO_2:NOx Balanced**	**NO_2:NOx High**
NH_3:NOx Low	Preferential ΔNO_2	Proportionate, or, Preferential ΔNO_2	Restricted ΔNO_2
NH_3:NOx Stoichiometric	Preferential ΔNO_2	Preferential ΔNO_2	Proportionate
NH_3:NOx High	Preferential ΔNO_2	Preferential ΔNO_2	Proportionate

The effect of brick length is most apparent in Fig. 3 for NO_2:NOx ratios 0.46 and 0.62 when the ammonia supply is adequate or in excess. It is also seen when NO_2:NOx is small, 0.05, although the NO_2 values are very low in this case and the uncertainties in the measured ratios are consequently higher. At high NO_2:NOx ratio, however, the effect of brick length appears minimal.

5 MEASUREMENTS FROM TEST EXHAUST COMPARED WITH STEADY-STATE CFD SIMULATIONS

5.1 Measurements at 220°C

The data are presented as conversion efficiencies in Figs. 4 to 6, and compared with CFD simulations. Fig. 4 shows measured and predicted NOx conversion efficiencies for different inlet NO_2:NOx ratios. Agreement between measurements and predictions is moderate for NO2:NOx near 0.46 and 0.62. When NO2:NOx was very low, near 0.05, NOx conversion is over-predicted, but in the case where NO2:NOx is high, near 0.82, NOx conversion is quite well predicted when there is an adequate or excess supply of ammonia, NH_3:NOx equal to or greater than 1.0.

The details of the predictions are explored in Figs. 5 and 6 where NO, NO_2 and NH_3 conversion are considered separately. Fig. 5 shows conversion efficiencies for NO_2:NOx ratios 0.62 and 0.82. For 0.82 there is under-prediction for conversion of all three species in the deficient ammonia case. Closest agreement is seen in the stoichiometric case. In the excess ammonia case, NO_2 conversion is well predicted but NO and NH_3 conversion are over-predicted. For 0.62, conversion of all three species is under-predicted in the deficient ammonia case. Agreement is fair in the stoichiometric case. Conversion is in general over-predicted in the excess ammonia case although agreement is much better at 91 mm than at 30 mm and 45 mm.

The case shown in Fig. 6 where the NO_2:NOx ratio is slightly lower, 0.46, is similar to the 0.62 case in Fig. 5. Agreement is fairly good in the stoichiometric case. In the deficient ammonia case, NO conversion is well predicted but NO_2 and ammonia

conversion efficiencies are both drastically under-predicted. In the excess ammonia case, NO and NH_3 conversion are over-predicted except at 91 mm where data and predictions agree fairly well. NO_2 predictions agree better with the data, notably at 75 and 91 mm.

Fig. 6 also shows the case for NO_2:NOx 0.05, where NOx was composed mostly of NO. Conversion of NO_2 is over-predicted in the deficient ammonia case, but it is only present in small quantity. Conversion of NO and NH_3 are also both over-predicted. All species are over-predicted in the stoichiometric case and the excess ammonia case.

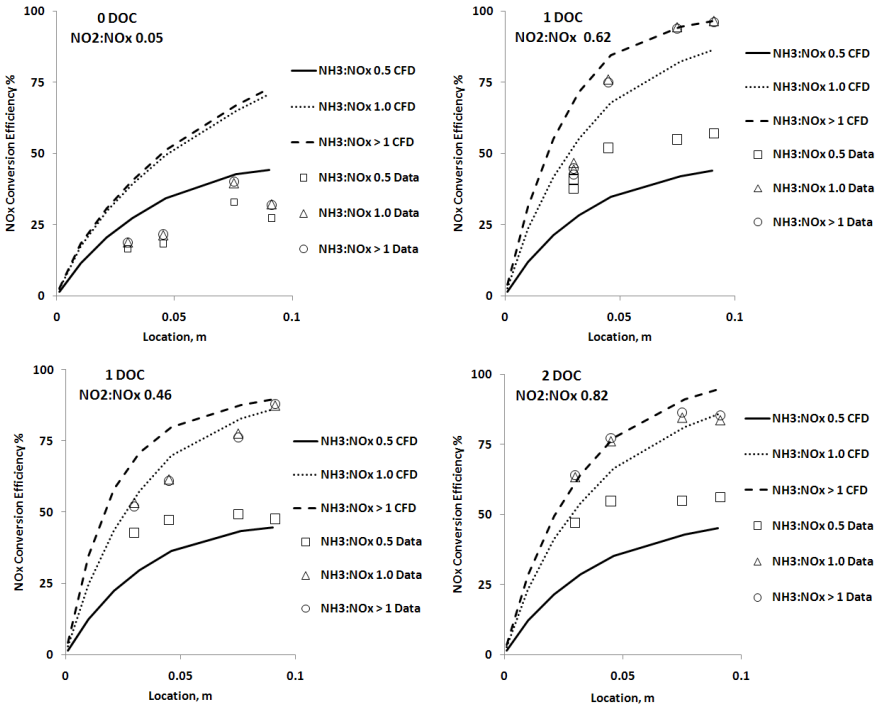

Figure 4: Measured and predicted NOx conversion efficiencies for cases with NO_2:NOx ratios 0.05, 0.46, 0.62 and 0.82.

For the cases with higher levels of NO_2, ratios 0.82 and 0.62, Fig. 5, the conversion is under-predicted in the deficient ammonia cases and over-predicted in excess ammonia cases. This is consistent with inhibition of the reactions by excess ammonia and promotion of the reactions by excess NOx relative to the standard Olsson scheme used for the kinetics in the CFD model. The 0.46 ratio tests, Fig. 6, suggest a similar scenario. For the case with ratio 0.05, Fig. 6, where the NOx was mainly NO, this pattern is less apparent as there is universal over-prediction of conversion efficiency.

The observations could suggest that under excess NOx conditions, there is a higher probability of a NOx molecule occupying an active site first, which may be a pre-

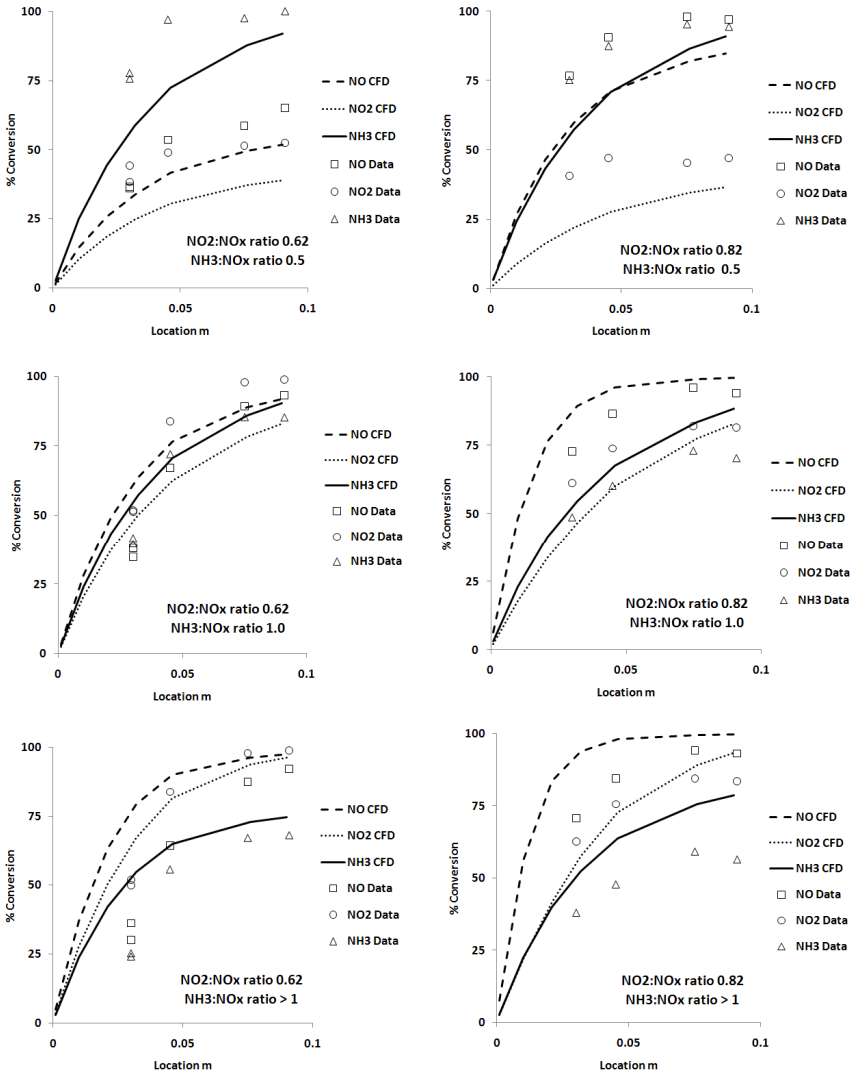

Figure 5: Conversion efficiency data for NO, NO_2 and NH_3 compared with CFD predictions for NO_2:NOx ratios 0.62 and 0.82.

condition for reaction. Under excess ammonia conditions, it is probable that the site will first be occupied by an ammonia molecule and this could block the site and inhibit the reaction. The Olsson et al. model (3) considers only one type of site, on to which ammonia is adsorbed, and on which the reactions take place. An additional term in each reaction rate dependent upon the local NOx:NH_3 ratio could adjust the reaction rates to make an allowance for the rate enhancement or rate inhibition effect. The inhibition effects here are attributed to site blocking, although Grossale et al. (14) in a study of iron zeolite attributed it to ammonia capturing a key intermediate species in the reaction scheme, so that the reaction with NO was unable to proceed.

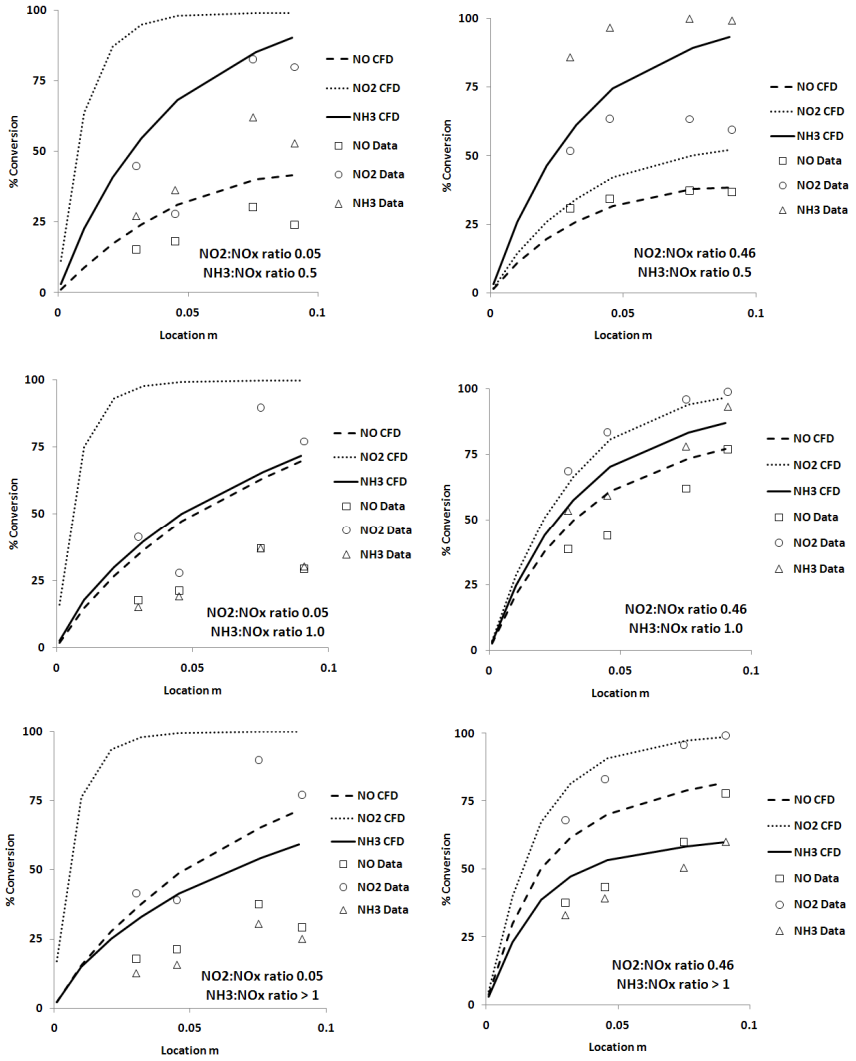

Figure 6: Conversion efficiency data for NO, NO_2 and NH_3 compared with CFD predictions for NO_2:NOx ratios 0.05 and 0.46.

In the model all the calculated reaction rates depend upon Ω mol sites/m^3 monolith, which is normally a constant. If the rates are multiplied by a function that, in effect, enhances or depletes the number of mol sites in proportion to the local NOx:NH_3 ratio then the reaction rates would be adjusted to account for site occupancy. This would in turn affect the fraction of sites occupied determined from equation (10). Preliminary trials of this modification have improved agreement between data and CFD predictions in some cases but have not provided universal improvement. The ammonia adsorption/desorption kinetics also influence all the SCR reaction rates and this may also require adjustment. Development work on these aspects of the model is ongoing.

5.2 Measurements at 300 °C

The data obtained in the higher temperature measurements are presented as conversion efficiencies in Figs. 7 and 8 and compared with CFD simulations. Fig. 7 shows NOx conversion is universally under-predicted for these tests. Fig. 8 shows the details as NO, NO_2 and NH_3 conversion. When ammonia is deficient, all three species are under-predicted, even at 91 mm from the brick inlet. Clearly in the experiment the conversion rates are very high near 300 °C and almost all ammonia is converted or stored within 30 mm from the brick inlet. NO conversion exceeds NO_2 conversion after 45 mm in the deficient ammonia case. NO_2 conversion does not rise significantly after 30 mm but NO conversion is still increasing at 91 mm.

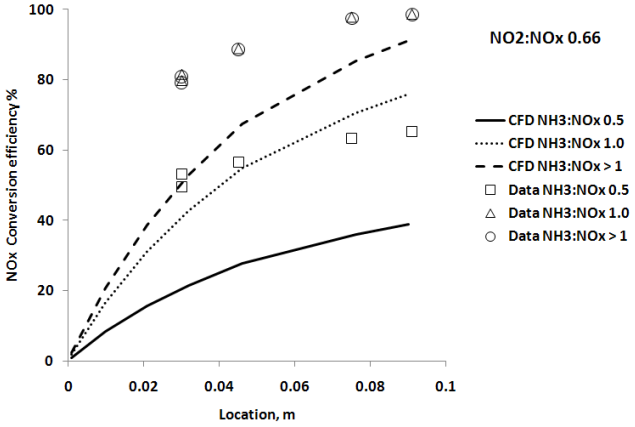

Figure 7: NOx conversion efficiency, measured and predicted, at 300 °C.

When stoichiometric ammonia is supplied, again the rates of conversion are higher than predicted. The conversion efficiency is the same for NO and NO_2 in the experiments but conversion efficiency is predicted to be much higher for NO than for NO_2. Ammonia conversion efficiency agrees approximately with predictions at 91 mm but is under-predicted for shorter lengths.

When excess ammonia is supplied, the measured conversion efficiency for NO and NO_2 is again very similar. The predictions of NO conversion are approximately correct but NO_2 conversion is significantly under-predicted. Ammonia conversion efficiency is predicted correctly at about 60 mm but under-predicted at shorter lengths and over-predicted at longer lengths.

Overall agreement between measurements and predictions for the three different ammonia input levels is poor; the model has only limited ability to predict the observed data at this temperature.

Comparison of Fig. 8 for NO_2:NOx 0.66 with Fig. 5 for NO_2:NOx ratio of 0.62 suggests that the predictions are generally better near 220°C than 300°C. The discrepancies between data and predictions at the two different temperatures suggest it is likely that the temperature dependence of the reaction rates is in need of modification. This is in addition to other aspects of the reaction rate kinetics

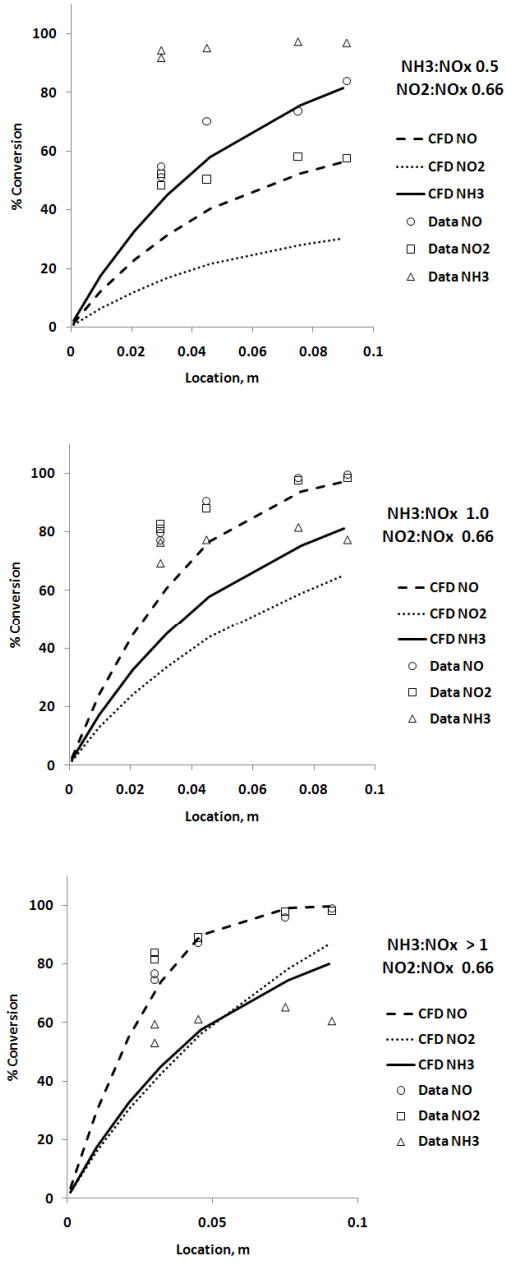

Figure 8: Measured conversion efficiencies for NO, NO_2 and NH_3 compared with CFD predictions for 300 °C engine tests.

discussed earlier. At the higher temperature, Figs. 7 and 8, an excess of NOx has promoted the reactions for NH_3:NOx ratio near 0.5 but an excess of ammonia does not appear to have inhibited the reactions.

6 CONCLUSIONS

Model validation data have been obtained for NO, NO_2 and NH_3 conversion with SCR brick lengths between 30 and 91 mm. Tests were carried out at 220 °C and 300 °C. A range of NO_2:NOx ratios was investigated between 0.05 and 0.82. The space velocities in the engine tests described in this paper were very much higher than those in the reactor experiments (3) on which the kinetic model was based. The measurements obtained in this study were real engine exhaust test data and so the study reported here provides a very strong test of the kinetic model.

Analysis of the measured NO:NOx and NO_2:NOx consumption ratios for the 220 °C tests showed that for 0.82 NO_2:NOx ratio, NO and NO_2consumption was proportionate for cases where ammonia supply was adequate or excess but there was relatively more NO_2 consumption and less NO consumption when the ammonia supply was deficient. For 0.46 and 0.05 NO_2:NOx ratios, NO_2 consumption was high and NO consumption was low whether ammonia supply was deficient or excess. For 0.62 NO_2:NOx ratio the same was true for adequate and excess ammonia but the consumption of NO and NO_2 was proportionate when the ammonia supply was deficient.

Comparison of the data with predictions from a CFD model based on Olsson kinetics (3) showed that the model provided in general an overall description of the data but that in detail there were many discrepancies. The best description provided by the model was for NO_2:NOx ratios of 0.46 and 0.62 and a stoichiometric supply of ammonia at 220 °C. Agreement was generally better at brick lengths of 91 mm and poorest for the shortest brick, 30 mm.

At 220 °C there was a tendency, most noticeable for NO_2:NOx ratios of 0.46 and 0.62, for cases where excess ammonia was supplied to be over-predicted by the CFD model and where deficient ammonia was supplied for levels to be under-predicted. This was most noticeable for short brick lengths and suggested that excess NOx promoted reactions whereas excess ammonia inhibited reactions.

Attempts to modify the CFD model to improve agreement of measurements and predictions are ongoing. Comparison of studies at 220°C and NO_2:NOx ratio 0.62 with those at 300 °C and NO_2:NOx ratio 0.66 also suggests that the temperature dependence of the kinetics is in need of modification.

REFERENCE LIST

(1) M. Schwidder, S. Heikens, A. De Toni, S. Geisler, M. Berndt, A. Bruckner, W. Grunert. The role of NO_2 in the SCR of nitrogen oxides over Fe-ZSM-5 catalysts: Active sites for the conversion of NO and NO/NO_2 mixtures. *Journal of Catalysis* 259 (2008) 96 – 103

(2) K. Kamasamudram, N. W. Currier, X. Chen, A. Yezerets. Overview of the practically important behaviors of zeolite-based urea-SCR catalysts, using compact experimental protocol. *Catalysis Today* 151 (2010) 212 – 222

(3) L. Olsson, H. Sjovnall, R. Blint. A kinetic model for ammonia selective catalytic reduction over Cu-ZSM-5. *Applied Catalysis B: Environmental* 81 (2008) 203-217

(4) J.N. Chi, H.F.M. Da Costa. Modeling and control of a urea-SCR after-treatment system. SAE Technical Paper 2005-01-0966

(5) D. Chatterjee, T. Burkhardt, M. Weibel, I. Nova, A. Grossale, E. Tronconi. Numerical simulation of Zeolite and V-based SCR catalytic converters. SAE Technical Paper 2007-01-1136

(6) K. Narayanaswamy, Y. He. Modeling of Copper zeolite and iron zeolite SCR catalysts at steady state and transient conditions. SAE Technical Paper 2008-01-0615

(7) S.F. Benjamin, C.A. Roberts. Three-dimensional modelling of NOx and particulate traps using CFD: A porous medium approach. *Applied Mathematical Modelling* 31 (2007) 2446-2460

(8) J-Y Luo, X. Hou, P. Wijayakoon, S. J. Schmieg, W. Li and W.S. Epling. Spatially resolving SCR reactions over a Fe/zeolite catalyst. *Applied Catalysis B: Environmental* 102 (2011) 110- 119

(9) T. C. Watling, M. Tutuianu, M. R. Desai, J.Dai, P. Markatou, A. Johansson. Development and validation of a Cu-Zeolite SCR catalyst model. SAE Technical Paper 2011-01-1299

(10) M. P. Sturgess, S. F. Benjamin, C. A. Roberts. Spatial conversion profiles within an SCR in a test exhaust system with injection of ammonia gas modeled using the porous medium approach. SAE Technical Paper 2010-01-2089

(11) S.D. Shah, A. Mauti, J.F.O. Richert, M.J. Loos, R.E. Chase. Measuring NOx in the presence of ammonia. SAE Technical Paper 2007-01-0331.

(12) R. K. Shah, A. L. London. Laminar forced flow convection in ducts. Academic Press Inc. (1978)

(13) N. Kapas, T. Shamim, P. Laing. Effect of mass transfer on the performance of SCR systems. *ASME J Eng Gas Turbines and Power* 133 Issue 3 (2011) Article number 032801

(14) A. Grossale, I. Nova, E. Tronconi. Ammonia blocking of the fast SCR reactivity over a commercial Fe-zeolite catalyst for diesel exhaust after-treatment. *J. Catalysis* 265 (2009) 141-147

CONTACT INFORMATION

S. F. Benjamin
s.benjamin@coventry.ac.uk

ACKNOWLEDGMENTS

Robert Gartside of Coventry University provided invaluable technical assistance with the engine testing. The authors are grateful for technical support from Faurecia, Jaguar-Land Rover, and Johnson Matthey plc. Funding for the research programme has been provided by EPSRC, UK.